Palm leaf ash as a biosorbent for improving the efficiency of the silver removal process
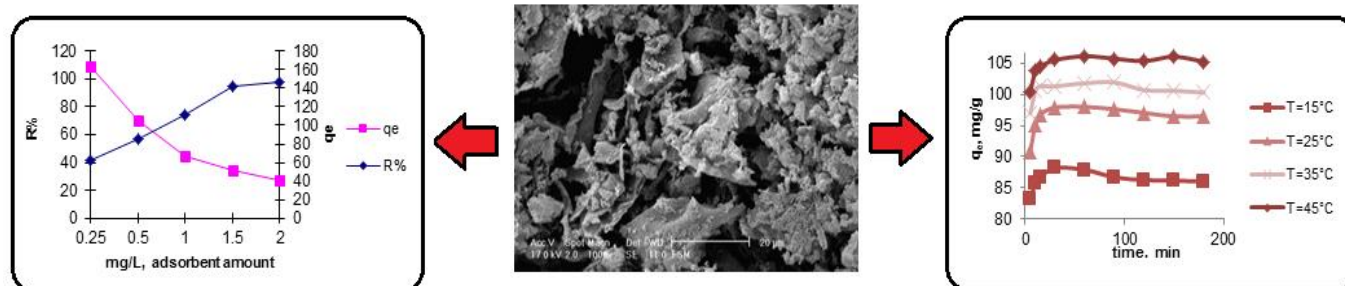
Elahe Ahmadi Kamarposhti[1] , Nader Bahramifar[*,2] , Salma Ehsani Tilami[3]

[1]Department of Chemistry, Payame Noor University, Sari, Iran.
[2]Department of Environmental Sciences, Faculty of Natural Resources, Tarbiat Modares University, Noor, Iran.
[3]Department of Basic Science, Farhangian University, Tehran, Iran.

GRAPHICAL ABSTRACT

ABSTRACT

Water pollution caused by heavy metals due to the increasing growth of industries is very worrying. Among heavy metals, evaluating the effect of silver (Ag) toxicity and its challenges on human and environmental health is very important and fundamental. This paper, for the first time, assessed the ability of palm leaf ash (PLA) as a biosorbent to reduce the amount of water-soluble Ag cations from water. To do so, the effect of adsorbent amount, contact time, initial concentration of Ag ions, pH of the solution, and the temperature was evaluated on the adsorption process. The adsorption process was more consistent with the Freundlich isothermal model and the pseudo-second-order model was in better agreement with experimental data. The results of the experiments showed that the removal percentage of Ag ions and adsorption capacity was accrued from 91.84 to 99.94% and from 25.89 to 52.771 mg/g with increasing pH from 3 to 8 respectively and the enthalpy of the adsorption process (ΔH) was 6996.36 j/mol. Furthermore the removal efficiency of Ag at the initial concentration was obtained at 99.7%, Therefore, it can be concluded that cheapness, and abundance and high sorption capacity are the main advantages of this adsorbent.

1. Introduction

Generally, studying heavy metals is important from two aspects: from a health point of view and an ecological point of view (Eisapour Chanani et al. 2015; Rangabhashiyam et al. 2019). Unlike their compounds, heavy metals as persistent contaminants cannot be degraded by biological or chemical processes in nature (Azizi et al. 2016; Falsafi et al. 2020; Heidarzadeh et al. 2020). Increasing industrial activities in recent years have led to an increase in the concentration of heavy metals in the environment, especially in the aquatic ecosystem. Heavy metals are discharged from various industries such as plating, textile, and electrical industries (Wang et al. 2010). Silver (Ag) is a metal that is widely used in various industries due to the conductivity of electricity and heat, ductility, and antimicrobial properties (Ahmadi. 2020). The most important uses of this metal are for coining, mirroring, jewelry making, and for preparing silverware, silver halides in photography and dental amalgams (Jeon

2017) Excessive amounts of Ag are discharged into industrial wastewater. Wastewater containing Ag higher than standard due to its toxic effect on the liver, heart, and lung causes adverse effects including cancer, heart failure, and genome variation on the human body and environment. Therefore, it is essential to develop effective methods for Ag recycling and improve the quality of this process for which generally the methods as electrolysis, ion exchange, membrane separation, and adsorption (Petrova et al. 2015).

Among all the routes and technologies including photochemical oxidation, chemical absorption, incineration, condensation, biological treatment, membrane, adsorption by solid absorbents like activated carbon and zeolite, the metal-organic frameworks (MOFs) are extensively developed owing to the ease of use and optimization potential related to the energy consumption and cost (zarei et al. 2020) The separation and recycling of Ag$^+$ were performed using several Tables such as silicon nanoparticles modified with sulfide groups (Zhang et al. 2017), active carbon (Song 2011), and coffee

*Corresponding author Email: n.bahramifar@modares.ac.ir

particles (Jeon. 2017). Low-cost, available, renewable, and eco-suitability characteristics have made scientists more interested in natural biosorbents (Nowrouzi et al. 2017; Nowrouzi et al. 2018; Thanut et al. 2015; Vassileva et al. 2016). In recent years, plant residues including rice husks, fern residues, corn bran and leaves, tobacco stems, sago palm residues, wheat bran, orange peel, and tea residues have been widely used to adsorb lead (Boudrahem et al. 2011; ; Fatyasari et al. 2020; Li et al. 2008; Qiantao et al 2018; Vesali-Naseh et al. 2021; Zulkali 2009). The results of a study have suggested that silica in rice husk, wheat bran, and palm ash adsorbs heavy metals (Rengga et al. 2020).

The palm tree is one of the most important species cultivated in the world. Due to the role and importance of palm in various fields and having advantages such as ease of use, short-term performance, low cost, less environmental pollution, its abundance and availability, today, its use as a biosorbent has been considered by biologists and researchers (Meijaard et al. 2018).

Thermodynamic or kinetic reaction control in a chemical reaction may determine the composition in the mixture of reaction products while competing pathways produce different products, and the conditions of reaction affect the stereo selectivity or selectivity. To remove pollutants via the adsorption method, the study of adsorption kinetics is very important and helps to understand the adsorption mechanism and steps that limit the speed of this process (Ouyang et al. 2019). In the adsorption process, the adsorbent behavior is analyzed by various kinetic models to determine the speed constants, initial adsorption speed, and adsorption capacity of the adsorbent (Kuang et al. 2020).

Based on the above mentioned, the aim of this study was to use PLA as an adsorbent to remove Ag from aqueous solutions in a batch system and to perform equilibrium and kinetic studies. To find the optimal conditions, the removal of some variables such as pH, temperature, adsorbent amount, and metal concentration was evaluated (the optimization process was carried out by one factor at the Time method (OFAT method) and the efficiency of Ag removal by PLA was compared with that by other adsorbents. In fact, the aim of this study aimed to prepare and use a cheap, abundant, and green adsorbent to absorb Ag from aqueous solutions.

2. Experimental
2.1. Materials and instruments

The leaves of Phoenix dactylifera belonging to the Arecaceae family were used in this research. Sodium hydroxide 97% and Ag chloride 97 % were purchased from Merck company and nitric acid 65 % for desorption process from Scharlu company. Identification and characterization of PLA were analyzed using X-ray fluorescence spectrometer Philips (XRF). The concentration of Ag ions was evaluated using an X-ray spectrometer and flame Atomic Absorption Spectrometer (GBC; Sens AA,). In addition, the surface morphology and structure of synthesized samples were carried out using scanning electron microscopy (SEM, Phillips XL30, Netherland).

2.2. Preparation of adsorbent

All experiments were performed in Payame Noor Research Laboratory in Sari**.** The palm leaves were washed, dried, powdered, burnt on an indirect flame, and converted into ash in a furnace at a temperature of 600 °C for 2 h, respectively. The produced ash was applied as an adsorbent to remove Ag⁺ cation in subsequent experimental.

3.3. Adsorption studies

To investigate the process of Ag removal from aqueous solutions, the study was done in a laboratory and batch systems. For adsorption studies on the adsorbent, the parameters of pH, adsorbent amount and concentration, contact time, and temperature were changed. First, 15 mL of 1000 mg/L metal cation solution was poured into a 250-mL Erlenmeyer; next, 135 mL of distilled water was added to it; after that, the solution pH was adjusted using NaOH and HNO₃. Then, some of the metal solutions were taken as a sample, and a certain amount of adsorbent was added to the erlenmeyer, placed inside a shaker-incubator with settings at 25 °C and 170 rpm. Then, the samples were taken at different intervals of 5, 10, 15, 30, 60, 90, 120, 150, and 180 minutes using a 0.2 µm Biofil syringe filter, and the concentration of Ag cations in collected solutions was measured by a flame atomic absorption spectrometer.

The effect of pH on the Ag adsorption amount was investigated using 100 mg of adsorbent at a pH range of 3-7 at 25 °C. To evaluate the effect of adsorbent dose on the adsorption process, different amounts of PLA were added to 150 ml solution containing Ag ions at 100 mg/L concentrations, optimum pH of 7 and 25 °C. Atomic absorption spectrometer (AAS) (GBC; Sens AA) was used to measure the concentration of metal ions in the test solution. The flame was rotated 35 degrees and the device was set at 338 nm for the Ag lamp. Initially, standard solutions with concentrations of 1, 10, 30, 50 and 70 were entered into the calibration device for both metal ions to draw the curve. After drawing the calibration curve by the device, the collected solutions at different times in the experiment were entered into the device from the higher times, respectively, and the concentration of Ag ions was measured based on the related calibration curve. The Ag calibration curve is shown as an example in Fig. 1.
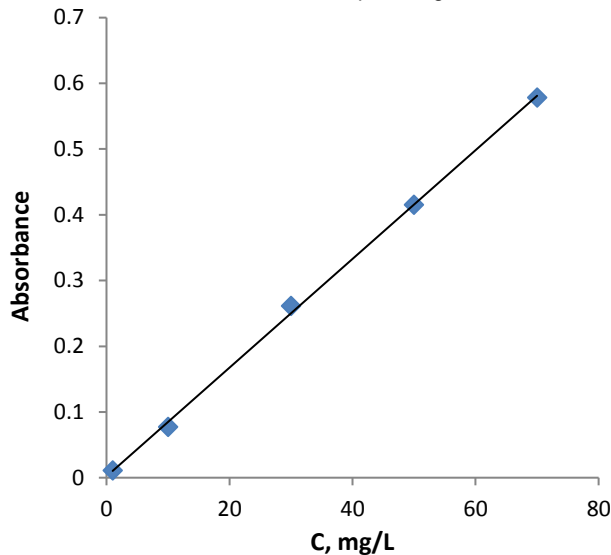

Fig. 1. Calibration curve obtained for measuring Ag cations by Flame AAS.

2.4. Equilibrium studies

In the present study, the effect of different concentrations of 50, 100, 150, 200, and 250 mg/Lwas assessed on the adsorption of Ag ions under optimal pH 7 and 2 g/Ladsorbent. Samples of the Ag solution were analyzed at certain intervals. The amount of surface adsorption at equilibrium (q_e) was calculated based on Eq. 1.

$$q_e = (C_\circ - C_e)/w \, V \tag{1}$$

q_e (mg/g): mg of metal ion adsorbed by one gram of PLA.
$C_\circ$: the initial concentration of the metal solution (mg/L).
C_e: equilibrium concentration of metal solution (mg/L).
V (mL): the volume of metal solution in tested Erlenmeyer.
W (g): the amount of PLA added to the tested Erlenmeyer.
Moreover, the percentage of metal ion removal was calculated by Eq. 2.

$$Removal \, (\%) = (C_\circ - C_e)/(C_\circ) * 100 \tag{2}$$

3. Results and discussion
3.1. Investigating the physical and chemical structure of PLA

In order to find the properties of the adsorption process, identification of the physical and chemical structure of the adsorbent is required. The physical properties of the adsorbent surface were also evaluated using SEM images (Fig. 2a). In this figure, the surface texture and morphology of the silica together with the accumulated silica are visible. The micrograph of the accumulated silica particles was exhibited with irregular shapes and different sizes. To understand the mechanism of the adsorption progress, FT-IR analysis was used to study the surface functional groups of PLA (Fig. 2 b). In figure 1b, the signals at 400-800 1/cm and 1100–1300 1/cm were assigned to Si–O–Si, and the bands at 1100 and 875 1/cm were attributed to the stretching and asymmetric bend vibrations of Si–O–Si, respectively (Wannapeera et al. 2008). Moreover, a broad band at about 3400 1/cm was assigned to the stretching vibrational band of the hydroxyl (–OH) group (Biswas et al. 2016). The presence of porous surfaces leads to an increase in the surface-to-volume ratio, resulting in an enhancement in adsorption. Figure 2c displays the X-ray diffraction

(XRD) Spectrum of the extracted silica, which has a wide peak at Bragg angles of 22°-23°.
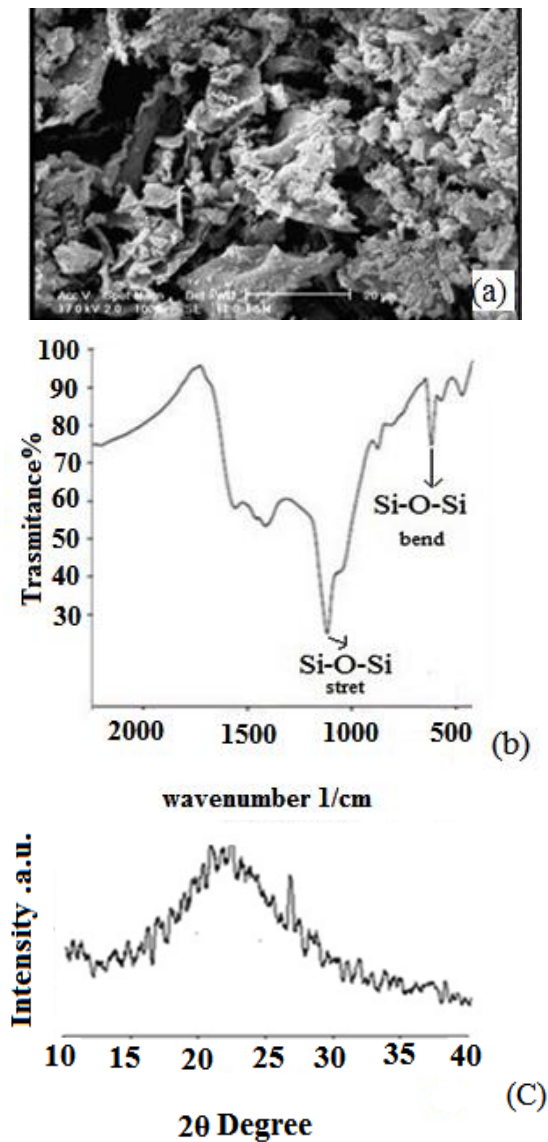

Fig. 2. (a) SEM images of palm ash after leaching treatment in 600 °C, (b) FT-IR Spectra of Palm leaf ash (c) XRD pattern of adsorbent.

3.2. Effect of pH on adsorption

Fig. 3 illustrates the effect of pH on the Ag adsorption amount at levels of 3, 4, 5, 6, 7, and an initial concentration of 100 mg/L. The aqueous solution pH as one of the most important controller parameters in the adsorption process can affect the removal percentage and adsorption capacity due to the effectiveness on the solubility of metal ions, the density of ions on the surface of the functional group, and ionization degree of adsorbent during the reaction. The results of the experiments showed that the removal percentage of Ag ions and adsorption capacity was accrued from 91.84 to 99.94 % and from 25.89 to 52.771 mg/g irregularly with increasing pH from 3 to 8 respectively. The highest adsorption percentage was related to pH 7 at 2 g/L adsorbent dose. At low pH (pH < 4) the cell wall surface of the adsorbent was protonated and had a positive charge and H^+ ions competed with Ag cations for active sites of an adsorbent. As a result, at low pH, the adsorption capacity was reduced while the negative charge potential at the adsorbent surface and adsorption capacity of Ag ions were increased at higher pH (pH >4). pH 7 at 2 g/L adsorbent dose was selected for future studies.

3.3. Evaluating the effect of biosorbent dose on cations' adsorption

As shown in Fig. 4, the percentage of metal ion removal is increased by raising the adsorbent dose so that the increase of PLA amount from 0.25 g/L to 2 g/L enhances the removal percentage from 41.48 to 99.94 % and decreases the adsorption capacity from 164.11 to 41.047 mg/g.
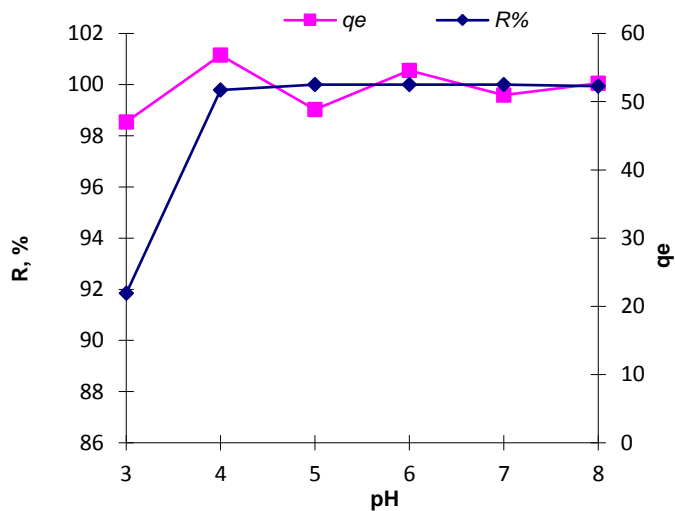

Fig. 3. Effect of pH on Ag removal; conditions: adsorbent dose=2 mg/L, initial concentration=100 mg/L, agitation time=180 min at 500 rpm and 25 °C.
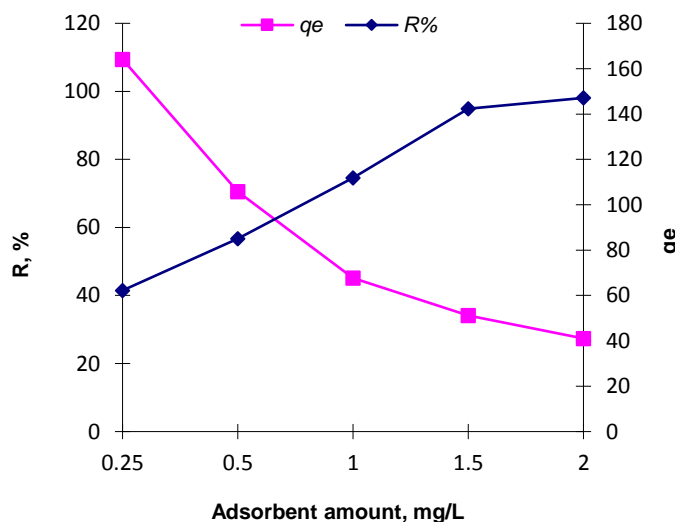

Fig. 4. The effect of adsorbent amount, conditions: Ag⁺ initial concentration=100 mg/L, pH= 8 and temperature=25 °C.

The reason for increasing the removal percentage by adding the adsorbent dose can be attributed to that increasing the adsorbent concentration due to the increase of active sites at its surface provides more space for adsorption; therefore, the penetration of metal ions into adsorption sites is easier. By comparing the amounts of adsorbent consumption for Ag ions, it was observed that the optimum amount of adsorbent for Ag cations was 2 g/L with a removal percentage of 99.94 %.

3.4. Effect of the initial concentration of metal ion

The initial concentration can play a role in the driving force necessary to overcome the ionic mass-transfer resistance between the adsorbent and liquid phase. To investigate the effect of the initial concentration of Ag ions on their removal using PLA, the initial concentration of Ag ions ranged from 50 to 250 mg/L, pH=7, and adsorbent dose=2 g/L were considered for Ag cations. The results of experiments in figure 5 illustrate the fact that as the concentration of metal ions rises, the removal efficiency is reduced but the adsorption capacity (q_e) of adsorbent is accrued so that the highest adsorption capacity of Ag ions is at 250 mg/L concentration. The higher initial concentrations enhance the mass-transfer driving force, leading to the adsorption increase. In addition, incrementing the concentration of

initial metal ions boosts the number of collisions between metal ions and adsorbent, which increases the adsorption process (Ebrahimi et al. 2019).
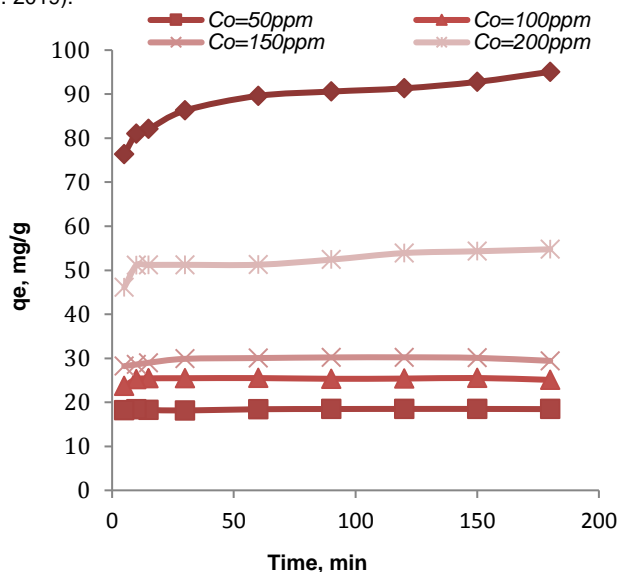

Fig. 5. Effect of initial concentration of Ag⁺, conditions: pH=7, adsorbent dose=2g/L and the initial concentration of Ag ions ranged from 50 to 250 mg/L.

3.5. Adsorption efficiency and temperature effect

Since temperature is an important parameter affecting the biosorption capacity in the adsorption process, the effect of temperature on the surface adsorption process was assessed for Ag metal solution at pH=7, adsorbent dose=2 g/L· and temperature ranges of 15, 25, 35, and 45 °C. The temperature effects in the thermodynamic studies of the adsorption process are shown in figure 6.
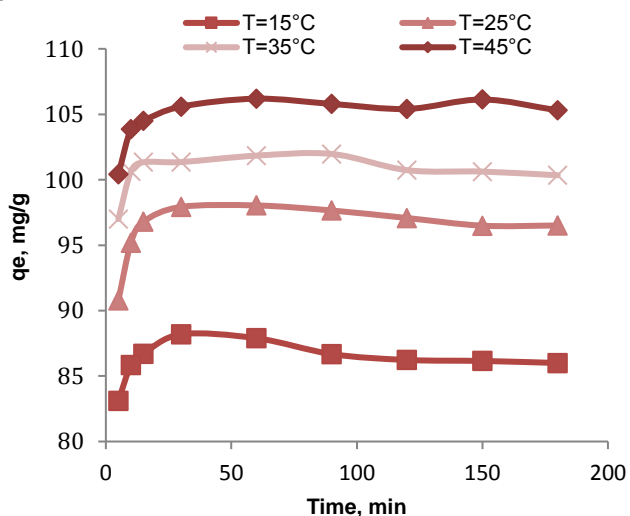

Fig. 6. The effect of temperature, conditions: adsorbent dose=2 g/L, pH= 8 and temperature ranges of 15, 25, 35 and 45 °C.

According to figure 6, because of the endothermic adsorption process, increasing system temperature, the adsorption capacity of Ag ions is enhanced, too. Nevertheless, at very high temperatures, the adsorption capacity was decreased due to the destruction of active sites and changing the nature of the adsorbent surface. Since it was possible to determine the surface adsorption process through studying the thermodynamic parameters such as Gibbs free energy (ΔG), enthalpy (ΔH), and entropy (ΔS), the van't Hoff equation was used to obtain the values of these parameters (Equation 3). Where R is the gas constant equal to 314.8 J/mol k and T is the Kelvin temperature. The values of thermodynamic parameters could be calculated using van't Hoff equation (drawing the plot of LnkD versus 1/T).

$$\log \frac{qe}{ce} = \Delta s° / 2.303R + (-\Delta H)/2.303R$$
$$(\Delta H) = (\Delta G - T \Delta S) \qquad (3)$$

The positive and negative enthalpy indicated the endothermic and exothermic adsorption processes, respectively. The positive entropy represented an extreme dependence of adsorbent and pollutants on adsorbing. Furthermore, the Gibbs free energy expressed the spontaneous reaction of the adsorption process (Olivotos and Economou-Eliopoulos 2016) The obtained (ΔG), (ΔH), and (ΔS) values are presented in Table 1. The enthalpy change (ΔH) suggests the bond strength, which determines the endothermic and exothermic adsorption process. The positive entropy (ΔS) indicates the increase of disorder at the solid-solution interface during adsorption, resulting in the growing trend of reaction disorders. As illustrated in Table 1, the obtained (ΔG) gets more negative with increasing the temperature, indicating that the spontaneous reaction escalates at high temperatures. Regarding the obtained values in Table 1, the heat of surface adsorption for Ag cation is 6996.36 j/mol, which considering that the heat of surface physical adsorption is less than 10 kcal/mol represents that the process of Ag ions adsorption using PLA adsorbent is a physical surface adsorption process.

Table 1. Thermodynamic parameters for adsorption of Ag ions by PLA.

Temperature, K	$\Delta G°$, j/mol	$\Delta H°$, j/mol	$\Delta S°$
288	−12871.896		
298	−13561.766	6996.36	68.987
308	−14251.636		
318	-14941.506		

3.6. Desorption study

The adsorption and desorption processes were performed for Ag ions at a concentration of 100 mg/L, and solutions of 1 M, 0.1 M, 0.01 M, and 0.001 M HNO₃ were used to obtain the desorption amount of Ag ions. Based on the results obtained in the adsorption process, the adsorption capacity was enhanced with increasing pH in the range from 5 to 8, but the best performance of the desorption process occurred in the acidic range because at acidic pHs (low), the adsorbent surface was protonated and the repulsive force between positively charged surfaces and Ag cations was increased. Fig. 7 represents desorption for Ag ions. As shown in Fig. 7, the Ag ion is desorbed at low pHs. Ag ion had the highest desorption at 1 M acid concentration because the adsorption process approximately occurred in the basic environment; as a result, the Ag ion returned to the acidic environment.
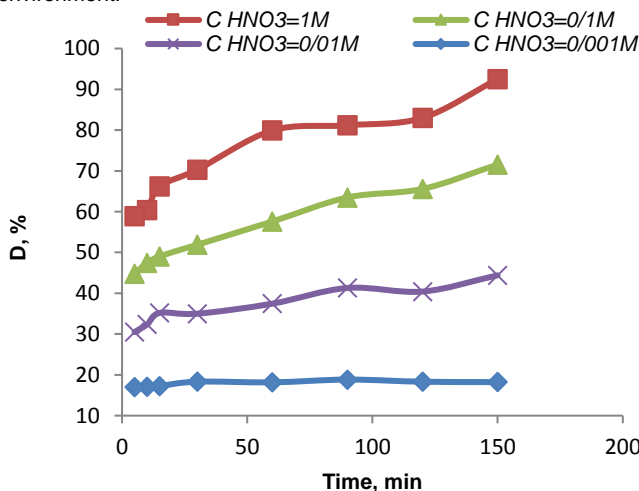

Fig. 7. Desorption for Ag ions by PLA adsorbent; conditions: initial Ag⁺ concentration=1g/L, pH= 7 and temperature=25 ℃.

3.7. Kinetic study of surface adsorption

In the current study, the linear form of pseudo-first-and-second-order kinetic equations was used to determine the adsorption rate of Ag ions. The pseudo-first-order kinetic model is used for reversible reactions that establish equilibrium between liquid and solid phases while the pseudo-second-order kinetic model assumes that the rate-controlling step may be chemisorptions. Kinetic studies of the adsorption process of Ag cations onto PLA were investigated at various equilibrium concentrations of a metal solution, at pH 7 and adsorption dose of 2 g/L. The plot of log (q_e-q_0) versus t for the pseudo-first-order kinetic model is illustrated in Fig. 8. The pseudo-first-order rate constants k_1 and q_e obtained based on slope and

intercept of log (q_e-q_t) versus t are presented in Table 2. Besides, the linear plot of t/qt versus t represented the pseudo-second-order kinetic plot (Fig. 9), and the pseudo-second-order rate constants k_2, q_e, and R^2 were obtained based on slope and intercept reported in Table 2.

Given that the obtained correlation coefficient values were closer to 1 and the calculated q_e was closer to experimental q_e, it could be concluded that the surface adsorption of Ag cation using PLA followed the second-order kinetic model.

Table 2. Comparison of kinetic constants of pseudo-first- and –second-order kinetic models at different concentrations for Ag+.

Initial concentration of the solution, mg/L	Pseudo first order kinetic model			Experiment, mg/g	Pseudo second order kinetic model		
	k_1 1/min	q_e mg/g	R^2		k_2 mg/g.min	q_e mg/g	R^2
50	0.0276	0.33	0.737	18.45	0.291	18.518	0.9999
100	0.04	0.656	0.527	25.593	0.152	25.64	0.9999
150	0.046	2.312	0.935	29.409	0.272	30.30	0.999
200	0.0069	5.272	0.484	54.788	0.00925	55.55	0.999
250	0.0115	15.488	0.949	95.077	0.0037	100	0.999

Freundlich isotherm model indicates heterogeneity of the adsorbent surface or surfaces with heterogeneous adsorption sites. In this model, KF values express the relative biosorption capacity and n is surface adsorption intensity (Togue Kamga 2019). In the Temkin model, the amount of adsorbed is related to the logarithm of the pressure of the adsorbate (Togue Kamga. 2019). The results of isotherm studies are listed in Table 3.

3.8. Comparison of adsorbent efficiency with other adsorbents

Various types of biological and non-biological substances can be used to remove heavy metals from water and wastewater. These substances include waste yeast, clay mineral composite, hydrolyzed lignocelluloses materials based on willow, and Table 4 demonstrates some of these substances and their efficiency in removing Ag. As represented in this table, clay mineral composite and palm leaf ash have the highest adsorption capacity by 69.93 and 52.771 mmol/g respectively but the removal efficiency of palm leaf ash is higher than clay mineral composite. In addition, the sorption ability of palm for adsorption of materials is compared in Table 5. As seen in this Table, the adsorption capacity of the studied adsorbent is significant compared to other adsorbents obtained from the palm.
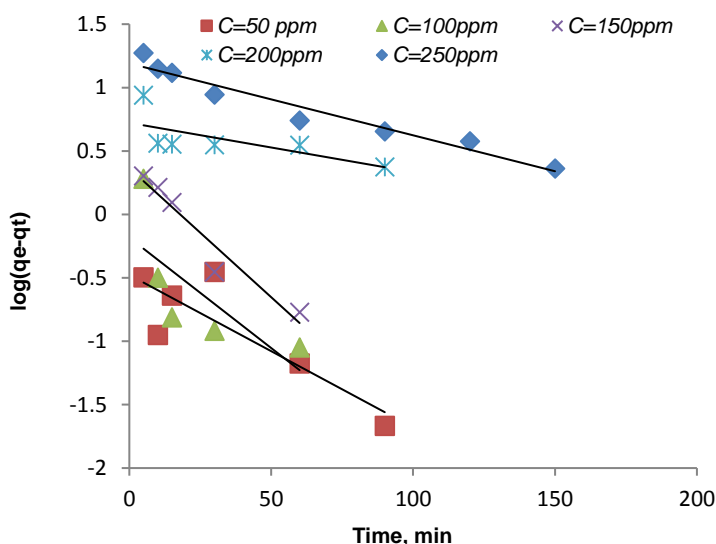
Fig. 8. log (q_e- q_t) versus t for the pseudo-first-order kinetic model.
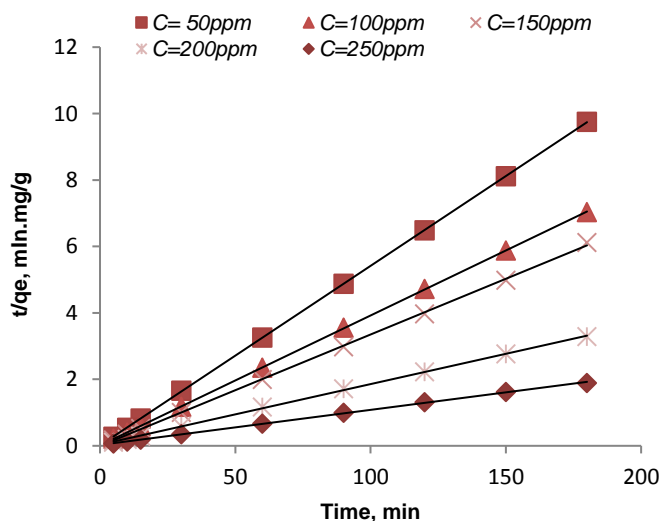
Fig. 9. The linear plot of t/q_t versus t for pseudo-second-order kinetic model.

Table 3. Constants of Langmuir, Freundlich and Temkin isotherm models for adsorption of Ag ions by PLA.

Temkin			Freundlich			Langmuir			
R^2	A	B	R^2	n	K_f	R_L	R^2	B, mg/L	q_m, mg/g
0.904	2.95	14.67	0.982	2.78	32.66	0.0072	0.93	0.55	**100**

Table 4. Some of substances and their efficiency in removing Ag^+.

Adsorbent	Maximum adsorption capacity	Removal efficiency	References
Waste yeast	41.8	> 93 %	(Yufeng et al. 2015)
Clay mineral composite	69.93	76.5 %	(Youness et al. 2019)
Hydrolyzed lignocellulosic materials based on willow	1.04	-	(Vassileva et al. 2016)
Hydrolyzed lignocellulosic materials based on paulownia	2.74	-	(Vassileva et al. 2016)
Hydrolyzed lignocellulosic materials based on wheat straw	2.53	-	(Vassileva et al. 2016)
Hydrolyzed lignocellulosic materials based on maize stalks	2.85	-	(Vassileva et al. 2016)
Chitosan/Montmorillonite Composite	43.48	-	(Thanut et al. 2015)
Chitosan	38.46	-	(Thanut et al. 2015)
Palm leaf ash	52.771	99.94 %	This work

Table 5. Comparison between the sorption ability of palm for adsorption of materials.

Sorbents structure	Adsorbed material	Adsorption capacity	References
African palm shells	CO_2	4.40	Ello et al. 2013
African palm	CO_2	5.05	Vargas et al. 2012
Iranian palm shell	Ag	52.77	This work

4. Conclusions

In the present study, surface adsorption of Ag ions by PLA biosorbent was performed to remove contamination caused by Ag metal in aqueous solutions. The results of the experiments showed that the highest adsorption percentage was related to pH 7 at 2 g/L adsorbent and an initial concentration of 250 mg/L. the removal efficiency of Ag at the initial concentration was obtained at 99.7 %. The heat of surface adsorption for Ag cation was 6996.36 j/mol, representing that the process of Ag ions biosorption using PLA adsorbent was a physisorption process. The results have indicated that this adsorbent has high efficiency for the removal of Ag ions. Based on this, other components of the palm can be used to prepare the adsorbent using the method mentioned in this article. The application of the prepared adsorbent in the removal of other heavy cations and dye from contaminated water is important and can be investigated.

Acknowledgments

References

Azizi S., Kamika I., Tekere M., Evaluation of heavy metal removal from wastewater in a modified packed bed biofilm reactor, PLoS ONE 11 (2016) e0155462.

Biswas R., Carpenter W., Voth G.A., Tokmakoff A., Molecular modeling and assignment of IR spectra of the hydrated excess proton in isotopically dilute water, The Journal of Chemical Physics 145 (2016) 154504-154516.

Boudrahem F., Aissani-Benissad F., Soualah A., Adsorption of lead(II) from aqueous solution by using leaves of date trees as an adsorbent, Journal of Chemical & Engineering Data 56 (2011) 1804–1812.

Ello A.S., de Souza L.K., Trokourey A., Jaroniec M., Development of microporous carbons for CO_2 capture by KOH activation of African palm shells, Journal of CO_2 Utilization 2 (2013) 35–8.

Eisapour Chanani M., Bahramifar N., Younesi H., Synthesis of Fe_3O_4@silica core–shell particles and their application for removal of copper ions from water, Journal of Applied Research in Water and Wastewater 4 (2015) 176-182.

Falsafi M.H., Moghaddas M., Moghaddas J.S., Removal of heavy metals from synthetic wastewater using silica aerogel- activated carbon composite by adsorption method, Journal of Applied Research in Water and Wastewater 7 (2020) 89-95.

Fatyasari N.I., Wicaksoa D.R., Mirwana A., Irawana C., Ramadhania D., Ursulla., Selective adsorption of Pb(II) ion on amine-rich functionalized rice husk magnetic nanoparticle biocomposites in aqueous solution, Journal of Environmental Chemical Engineering 8 (2020) 129-134.

Heidarzadeh M., Abdi N., Varvani Farahani J., Ahmadi A., Toranjzar H., The effect of Typha Latifolia L. on heavy metals phytoremediation at the urban and industrial wastewater entrance to the Meighan wetland, Iran, Journal of Applied Research in Water and Wastewater 14 (2020) 167-171.

Kuang Y., Zhang X., Zhou S., Adsorption of Methylene Blue in Water ontoActivated Carbon by Surfactant Modification, water 12 (2020) 587-606.

Li W., Zhang L., Peng J., Li N., Zhang S., Guo S., Tobacco stems as a low cost adsorbent for the removal of Pb(II) from wastewater: Equilibrium and kinetic studies, Industrial Crops and Products 28 (2008) 294-302.

Meijaard E., Garcia-Ulloa J., Sheil D., Wich S.A., Carlson K.M., Juffe-Bignoli D., Brooks T.M. (eds.) Oil palm and biodiversity. A situation analysis by the IUCN Oil Palm Task Force. IUCN Oil: Switzerland; (2018).

Nowrouzi M., Younesi H., Bahramifar N., Superior CO_2 capture performance on biomass-derived carbon/metal oxides nanocomposites from Persian ironwood by H_3PO_4 activation, Fuel 223 (2018) 99-114.

Nowrouzi M., Younesi H., Bahramifar N., High efficient carbon dioxide capture onto as-synthesized activated carbon by chemical activation of Persian Ironwood biomass and the economic pre-feasibility study for scale-up, 168 (2017) 499-509.

Petrova Y.S., Pestov A.V., Usoltseva M.K., Neudachina L.K., Selective adsorption of silver(I) ions over copper(II) ions on a sulfoethyl derivative of chitosan, Journal of Hazardous Materials 299 (2015) 696–701.

Qiantao S., George E.S., Valentina P., Xiaoguang M., Mechanistic study of lead adsorption on activated carbon, Langmuir 34 (2018) 13565-13573.

Rangabhashiyam S., Jayabalan R., Rajkumar M. A., Balasubramanian P., Elimination of toxic heavy metals from aqueous systems using potential biosorbents: a review. In: Green Buildings and Sustainable Engineering, Springer: Singapore; (2019).

Rengga W.D.P., Sediawan W.B., Imani N.A.C., Harianingsih H., Salsabiil K.A., Adsorption studies of rice husk-based silica/carbon composite, Journal of Science and Data Analysis 2 (2020) 98-104.

Thanut J., Walaikorn N., Adsorption of Ag (I) from aqueous solution by waste yeast: kinetic, equilibrium and mechanism studies, Bioprocess and Biosystems Engineering 38 (2015) 69–77.

Togue Kamga, F., Modeling adsorption mechanism of paraquat onto Ayous (Triplochiton scleroxylon) wood sawdust. Applied Water Science 9 (2019) 1-7.

Vargas D.P., Giraldo L., Moreno-Piraján J., CO_2 adsorption on granular and monolith carbonaceous materials, Journal of Analytical and Applied Pyrolysis 96 (2012) 146-152.

Vassileva P.S., Radoykova T.H., Detcheva A.K., Avramova I.A., Aleksieva K.I., Nenkova S.K., Valchev I.V., Mehandjiev D.R., Adsorption of Ag^+ ions on hydrolyzed lignocellulosic materials based on willow, paulownia, wheat straw and maize stalks, International Journal of Environmental Science and Technology 13 (2016) 1319–1328.

Vesali-Naseh M., Vesali Naseh M.R., Ameri P., Adsorption of Pb (II) ions from aqueous solutions using carbon nanotubes: A systematic review, Journal of Cleaner Production 291 (2021) 125917-125927.

Wannapeera J., Worasuwannarak N., Pipatmanomai S., Improved Gasification of Rice Husks for Optimized Biochar Production in a Top Lit Updraft Gasifier, Songklanakarin Journal of Science and Technology 30 (2008) 393-404.

Youness R., Abdellah E., Allal M., Sophia K., Meriem A., Antonio G., Adsorption recovery of Ag(I) and Au(III) from an electronics industry wastewater on a clay mineral composite, International Journal of Minerals Metallurgy and Materials 26 (2019) 673–680.

Yufeng Z., Dongfang W., Hezhen X., Sung W.W., Longzhe C., Guiping W., Adsorption of Ag (I) from aqueous solution by waste yeast: kinetic, equilibrium and mechanism studies, Bioprocess and Biosystems Engineering 38 (2015) 69–77.

Zarei M.M., Moeinaddini M., Norouzi M., Rafiee R., Abbasi A.R., Facile and cost-efficient synthesis of highly efficient CO_2 adsorbents: a pathway towards a green environment, Journal of porous materials 27 (2020) 1-12.

Zhang L., Zhang G., Wang S., Peng J., Cui W., Sulfoethyl functionalized silica nanoparticle as an adsorbent to selectively adsorb silver ions from aqueous solutions, Journal of the Taiwan Institute of Chemical Engineers 71 (2017) 330–337.

Zulkali M.M.D., Ahmad A.L., Norulakmal N.H., Oryza S.L., Husk as heavy metal adsorbent: Optimization with lead as model solution, Bioresource Technology 97 (2009) 21-25.